Carbohydrate Polymers 103 (2014) 488–495

Contents lists available at ScienceDirect

Carbohydrate Polymers

journal homepage: www.elsevier.com/locate/carbpol

Structure analysis of a bioactive heteropolysaccharide from *Schisandra chinensis* (Turcz.) Baill

Ting Zhao[a], Guanghua Mao[b], Min Zhang[a], Weiwei Feng[b], Riwen Mao[c], Yang Zhu[a], Xiaoyun Gu[a], Qian Li[d], Liuqing Yang[a,*], Xiangyang Wu[e,**]

[a] School of Chemistry and Chemical Engineering, Jiangsu University, Xuefu Road 301, Zhenjiang 212013, China
[b] School of Food and Biological Engineering, Jiangsu University, Xuefu Road 301, Zhenjiang 212013, Jiangsu, China
[c] Nucell Biotechnology Co. Ltd., Jingsi Road 2, Zhenjiang 212009, Jiangsu, China
[d] School of Pharmacy, Jiangsu University, Xuefu Road 301, Zhenjiang 212013, Jiangsu, China
[e] School of the Environment, Jiangsu University, Xuefu Road 301, Zhenjiang 212013, Jiangsu, China

ARTICLE INFO

Article history:
Received 30 September 2013
Received in revised form
16 December 2013
Accepted 17 December 2013
Available online 6 January 2014

Keywords:
Schisandra chinensis (Turcz.) Baill
Polysaccharide
Structural elucidation
Chain conformation
Structure–activity correlation

ABSTRACT

Our previous study revealed that *Schisandra* polysaccharide (SCPP11) exerted excellent antitumor and immunomodulatory activities. In this investigation, the structure of SCPP11 was elucidated. The results indicated that SCPP11 has a backbone that is composed of 1,4-disubsituted-β-gal, 1,4-disubsituted-α-glu, 1,6-disubsituted-β-man and 1,4,6-disubsituted-α-gal. The branches was composed of 1,4-disubsituted-α-glu and 1-substitued-β-glu. The M_w and $(r_g^2)_z^{1/2}$ of the polymer molecules in 0.1 M NaCl were 1.793×10^4 Da and 11 nm, respectively. The exponent of $(r_g^2)_z^{1/2}$ versus M_w (0.39) suggested SCPP11 adopted a globular conformation with seldom random coil. Circular dichroism analysis revealed the presence of ordered structures in SCPP11. AFM and TEM further confirmed the agglomerated morphologies of SCPP11. In addition, it inferred the agglomerated conformation, branching structure and flexibility of chain are beneficial for exerting excellent activities. This information will be helpful in the recognition of biological systems for polysaccharides and the selection of active polysaccharide.

1. Introduction

Schisandra chinensis (Turcz.) Baill is in the Magnoliaceae family and have been extensively applied as traditional Chinese medicine and health food. Polysaccharide isolated from *S. chinensis* (Turcz.) Baill, as an important activated macromolecular, had been studied in some organizations (Chen, Tang, Wang, Sun, & Liang, 2012; Gao, Meng, Li, & Tong, 2009; Sheng, Liu, Huang, Yuan, & Guan, 2011; Tong, Zhao, Du, Tian, Feng, & Sun, 2012; Zao, Mao, Zhang, et al., 2013). However, these investigations mainly focus on the extraction, separation, preliminary characterization and activities of crude samples, while the repeating unit, conformation and the structure–activity correlation have not been reported. In our previous study (Zao, Mao, Mao, et al., 2013) a low molecular weight polysaccharide (SCPP11) was extracted and purified using DEAE-52 cellulose and Sephadex G-100 column from *S. chinensis* (Turcz.) Baill, and it exerted excellent antitumor and immunomodulatory function in *Heps*-tumor-bearing mice. Therefore, in this study, the structure analysis including chain conformation of SCPP11 was comprehensively analyzed by gas chromatography–mass spectrometry (GC–MS), nuclear magnetic resonance (NMR), high-performance size exclusion chromatography-angle laser light scattering-refractive index detector (HPSEC–MALL–RI), circular dichroism (CD), atomic force microscope (AFM) and transmission electron microscope (TEM), moreover, the preliminary discussion was conducted on the aspect of structure and antitumor and immunomodulatory function correlation. This information will be helpful in the recognition of biological systems for polysaccharides and the selection of active polysaccharide.

2. Materials and methods

2.1. Materials and reagents

The *S. chinensis* (Turcz.) Baill was obtained from Zhongxing Pharmaceutical Co., Ltd., Zhenjiang, Jiangsu Province, China. All other chemicals and solvents were of analytical reagent grade and were obtained from Sinopharm Chemical Reagent Co., Ltd. (Shanghai, China).

* Corresponding author. Tel.: +86 511 88791800; fax: +86 511 88791800.
** Corresponding author. Tel.:+86 511 88791200; fax: +86 511 88791200.
E-mail addresses: yangliuqing@ujs.edu.cn (L. Yang), wuxy@ujs.edu.cn (X. Wu).

0144-8617/$ – see front matter © 2013 Elsevier Ltd. All rights reserved.
http://dx.doi.org/10.1016/j.carbpol.2013.12.058

2.2. Methylation analysis

The SCPP11 was methylated three times by the method of Needs and Sevendran (Han et al., 2011; Needs & Selvendran, 1993; Pan et al., 2012; Scoparo et al., 2013) with slight modification. In brief, 5.0 mg of dry SCPP11 was added into the dried three-necked flask and dissolved in 2.0 mL of DMSO. When the SCPP11 was completely dissolved, the 100 mg dried NaOH was added. The mixture was then stirred for 1 h at room temperature (25 °C). After a majority of NaOH dissolved, 1.0 mL of methyl iodide was added for SCPP11 methylation. The sample was incubated in darkness for 4 h and then 2.0 mL of distilled water was used to decompose the remained methyl iodide. The methylated polysaccharides were extracted with 3× 2 mL of chloroform and then the chloroform layer was washed with distilled water for several times and vacuum-dried. The completeness of methylation was confirmed by the disappearance of the hydroxyl absorption in IR spectrum in 3400 cm^{-1}. The pre-methylated products were depolymerized with 85% formic acid at 100 °C for 6 h and further hydrolyzed with 2 M trifluoroacetic acid at 100 °C for 6 h. 25 mg of $NaBH_4$ was added to reduce the uronic acid. After incubation at room temperature for 12 h, the acetic acid was added to terminate the reduction. The partially methylated residues were dried under low pressure and than acetylated by 0.5 mL of acetic anhydride and 0.5 mL of pyridine. The reaction was kept at 100 °C for 1 h. The resulting partially methylated alditol acetates (PMAA) were extracted with methylene chloride and analyzed with GC–MS (6890N/5975B GC-MS, Agilent, USA), which equipped with a HP-5 column (0.25 mm × 30 m × 0.25 μm). The temperature was set as follows: the initial temperature of the column was 130 °C, maintained at 130 °C for 5 min, and then the temperature was increased to 240 °C at 4 °C/min. The 240 °C temperature was held for 5 min. PMAA were identified by their fragment ions in according to the MS spectrum and the relative retention time on GC profile.

2.3. NMR spectra

Exchangeable protons were replaced with deuterium by suspending a sample in D_2O and freeze-dried three times (Yang et al., 2011). All spectra including ^1H NMR, ^{13}C NMR, ^1H–^1H COSY, HMQC and HMBC were recorded on a Bruker DRX-400 spectrometer (Bruker, Rheinstetten, Germany) at 296.9 K. The scans number in ^{13}C NMR spectra was 25,000. Chemical shift was expressed in ppm.

2.4. HPSEC–MALL–RI measurements

HPSEC–MALL–RI system consists of a pump (1100 HPLC, Agilent, USA), and agilent 1100 injector (Agilent, USA) with a 100 μL injection loop, three HPSEC columns (OHpak SB-G, SB-803 HQ, SB-804 HQ and SB-805 HQ columns, Shodex, Tokyo, Japan), a MALLS detector (Wyatt Technology DAWN HELEOS-II, Wyatt Technology Co., USA), and a RI detector (1100 HPLC, Agilent, USA). The concentration of polysaccharide solution was 1.0 mg/mL. After passing through 0.22 μm syringe filters (Whatman, England), 100 μL polysaccharide solution was injected. The isocratic mobile phase was 0.1 mol/L sodium chloride at a flow rate of 0.4 mL/min. The *dn*/*dc* value of the SCPP11 sample in 0.1 mol/L aqueous NaCl was determined by OPTILAB DSP differential refractometer (Wyatt Technology Co., USA) at 633 nm and 25 °C to be 0.125 mL/g. The Astra software (Wyatt Technology Co., USA) was utilized for data acquisition and further analysis.

2.5. Circular dichroism

Circular dichroism spectra were recorded with a Jasco J-810-150s instrument in the wavelength region from 190 to 250 nm at room temperature. All solutions were filtered through 0.45 μm Millipore membrane before being used. Under different treatment conditions, the changes in circular dichroism spectra of polysaccharide were investigated. The various treatment conditions include different temperature (25, 60, 100 °C), different pH values (pH: 2.0, 6.5, 12.0) and different solvents (distilled water, calcium chloride solution, 6 mol/L Urea, Congo red solution). A correction for the solvent baseline was made digitally in each case.

2.6. Atomic force microscopy

SCPP11 were dissolved in distilled water to make a 1 mg/mL solution by energetic stirring for 24 h at room temperature and 100 °C, respectively, then diluted with distilled water to a concentration of 1 μg/mL and filtered through a 0.45 μm filter. A 5 μL drop was deposited on to freshly cleaved mica and dried for more than 1.5 h at room temperature. The specimen was examined using an MFP-3D atomic force microscope (MFP-3D, Asylum Research, American) under tapping mode in air (25 °C, relative humidity was 40–50%). The Nanoscope IIIa software (Version 5.30r3.sr3, Veeco Metrology) was used for image manipulation.

2.7. Transmission electron microscope

Molecular morphology of the SCPP11 specimen was performed on a high-resolution transmission electron microscope (JEM-2100, JEOL, Tokyo, Japan). The samples were dissolved in distilled water at concentration of 1 mg/mL, then energetically stirred for 24 h and filtered through a 0.45 μm filter. A drop of SCPP11 was deposited on to the electron microscope copper grids coated with a thin film of carbon. After dried at room temperature and atmospheric pressure, a drop of 0.2% phosphotungstic acid was used for the polysaccharide molecules staining. TEM images were taken at an accelerating voltage of 200 kV.

3. Results and discussion

3.1. Methylation analysis

The FT-IR spectrum of the methylated SCPP11 is shown in Fig. 1(A). The spectrum exhibits the characteristic IR absorption of polysaccharides at 1025–1152 cm^{-1}. At the same time, the hydroxyl absorption in 3400 cm^{-1} was disappeared and the absorption of C—H stretching vibration in 2900 cm^{-1} was strengthened, which indicated that the methylation reaction was completed.

The methylated SCPP11 was depolymerized and hydrolyzed by 85% formic acid and TFA, then acetylation. The individual peaks of the PMAA and fragmentation patterns were identified according to their retention time in GC and by comparison with literature (Carpita & Shea, 1989) and standard PMAA spectra patterns (Complex Carbohydrate Research Center, University of Georgia, USA). Based on the above analysis, the GC chromatogram of PMAA and the linkage patterns of SCPP11 were shown in Fig. 1(B) and Table 1, respectively. The results indicated that SCPP11 was composed of the residues of T-D-glu*p* (1→, →1)-D-gal-(4→, →1)-D-glu*p*-(4→, →1)-D-man*p*(6→ and →1)-D-gal*p*-(4,6→, as marked in Fig. 1(B). The molar ratio (Table 1) of each residue was derived from the peak area in the GC chromatogram. The proportion of the T-glu*p* residue is 12.20%. The important branch point is →1)-D-gal*p*-(6→substituted at 4-O positions, which accounts for 11.95%. The ratio between the apparent terminal units and branching point is 1.02, which is consistent with the fact that the number of polysaccharide branching points approximately equal to the number of terminal units. The unsubstituted residues were shown to

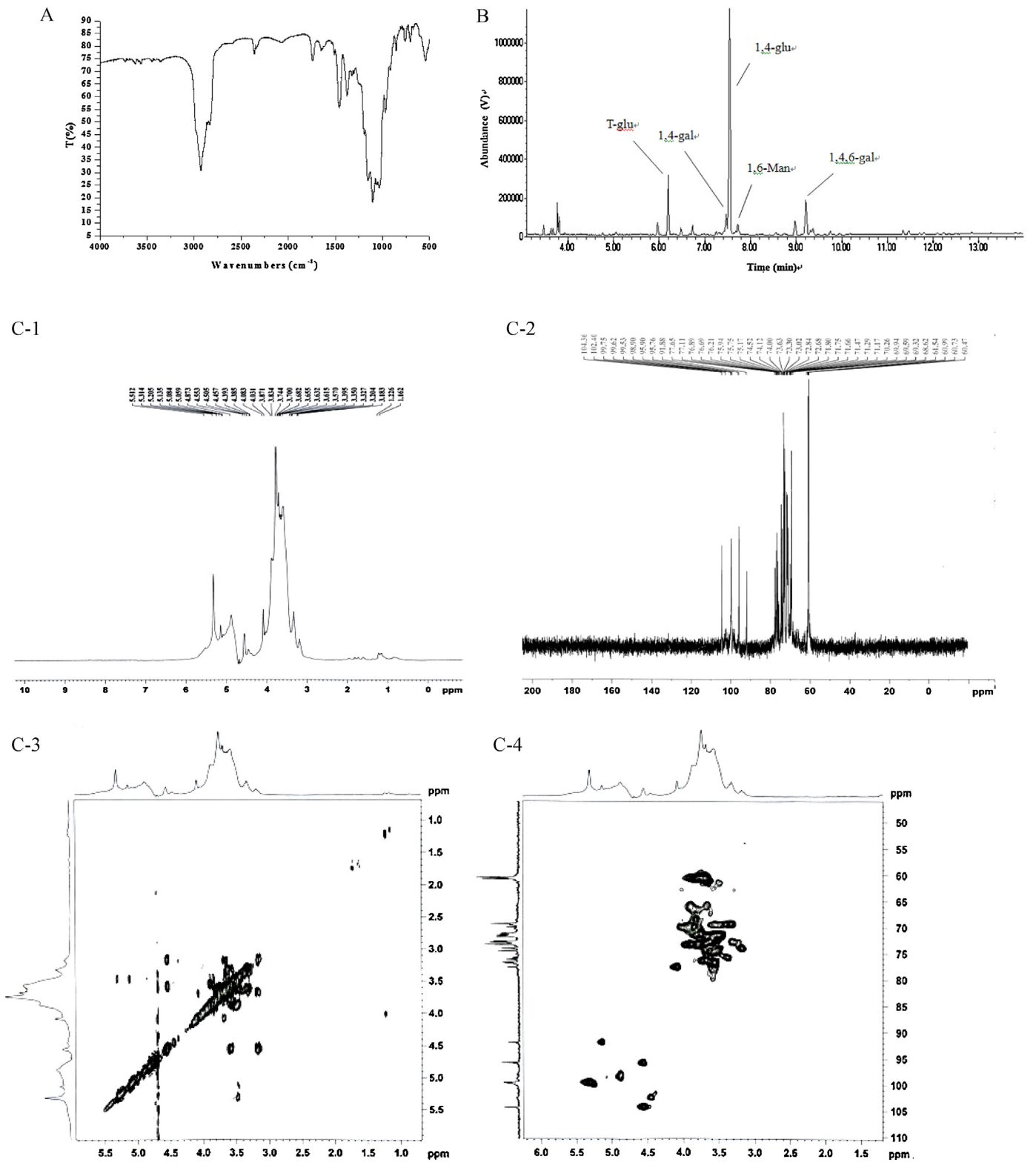

Fig. 1. (A) FT-IR spectrum of the methylated SCPP11 was recorded with a NEXUS 679 FT-IR spectrophotometer between 400 and 4000 cm^{-1} using the KBr-disk method. (B) The GC chromatogram from methylation analysis of SCPP11 fraction. The gas chromatography–mass spectrometer (6890N/5975B GC-MS, Agilent, USA), equipped with a HP-5 column (0.25 mm × 30 m × 0.25 μm) was used to analyze. The temperature was set as follows: the initial temperature of column was 130 °C, maintained for 5 min and then increased to 240 °C at 4 °C/min. The 240 °C was held for 5 min. (C) The NMR spectrum of polysaccharide SCPP11. The measuring temperature was 296.9 K. (C-1) The ^{1}H NMR spectra of SCPP11. (C-2) The ^{13}C NMR spectra of SCPP11. (C-3) $^{1}H/^{1}H$ COSY correlation spectra of SCPP11. (C-4) $^{1}H/^{13}C$ HSQC correlation spectra of SCPP11. (C-5) $^{1}H/^{13}C$ HMBC correlation spectra of SCPP11. (D) Chemical structure of polysaccharide SCPP11.

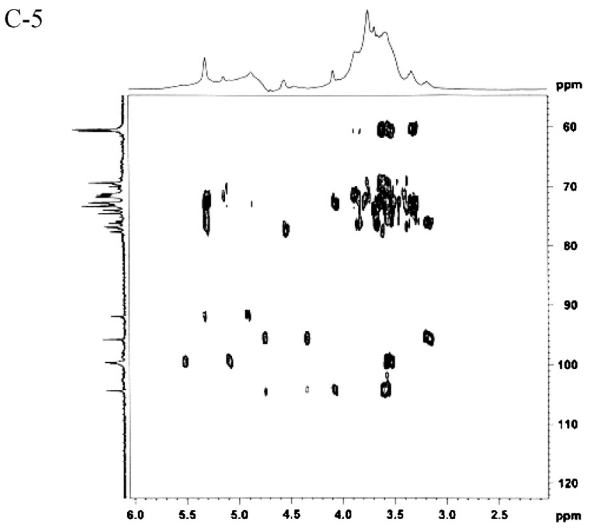

D

→{4)-α-D-Glc*p*(1}$_4$→{6)-α-D-Gal*p*(1}$_2$→6)-β-D-Man*p*(1→4)-β-D-Gal*p*(1→{4)-α-D-Glc*p*(1}$_4$→

4
↑
1

β-D-Glc*p*(1→4)-α-D-Glc*p*

Fig. 1. (*Continued*)

Table 1
Linkage analysis of the SCPP11 isolated from *Schisandra chinensis* (Turcz.) Baill.

Retention time (min)	PMAA	Linkage pattern	Ion fragmentation	Peak area percentage (%)	Molar ratio
6.17	2,3,4,6-Me$_4$-Glc*p*	T-Glc*p*	43, 59, 71, 87, 101, 117, 145, 161, 205	12.20	2.05
7.47	2,3,6-Me$_3$-Gal*p*	1,4-Linked-Gal*p*	43, 87, 101, 113, 117, 129, 131, 233	7.58	1.27
7.54	2,3,6-Me$_3$-Glc*p*	1,4-Linked-Glc*p*	43, 87, 101, 113, 117, 129, 131, 233	62.34	10.34
7.73	2,3,4-Me$_3$-Man*p*	1,6-Linked-Man*p*	43, 87, 101, 117, 129, 161, 189	5.92	1.00
9.22	2,3-Me$_2$-Gal*p*	1,4,6-Linked-Gal*p*	43, 87, 99, 101, 117, 129, 161, 189	11.95	2.00

be →1)-D-gal*p*-(4→, →1)-D-glu*p*-(4→ and →1)-D-man*p*(6→ in the proportion of 7.85%, 62.34% and 5.92%, respectively.

3.2. NMR analysis

The structural features of SCPP11 were further analyzed by the NMR spectra. According to the characteristic signals, the ^{1}H NMR and ^{13}C NMR spectra of SCPP11 were completely assigned according to two-dimensional COSY, HMBC and HMQC NMR analysis and on literature values, and the corresponding chemical shifts of signals were summarized in Table 2.

The ^{1}H NMR spectrum of SCPP11 was shown in Fig. 1(C-1). The signals at 5.0–5.4 and 4.4–5.0 ppm were assigned as the anomeric protons of α-glycosidical configuration and β-glycosidical configuration. It was in agreement with the IR results of SCPP11 conducted by Zao, Mao, Mao, et al. (2013). The high intensity signal at 5.31 ppm in the spectrum can be assigned to the signals of anomeric protons of α-1,4-D-Glc*p* (A). The chemical shifts at 5.14 ppm could be attributed to the anomeric protons of the α-1,4,6-D-Gal*p* (C). The three signals in the relative high field at 4.87, 4.51 and 4.53 ppm can be attributed to the anomeric protons of the β-terminal-D-Glc*p* (B), β-1,4-D-Gal*p* (D) and β-1,6-D-Man*p* (E), respectively. The all ^{1}H resonances in the ^{1}H NMR spectra could be assigned according to ^{1}H–^{1}H COSY (Fig. 1(C-3)) experiments and on literature values. In the residue A, the ^{1}H chemical shifts from the H-1 signal at δ 5.31 to H-2 at δ 3.48 and H-3 at δ 3.75 were clearly assigned. However, the assignments of H-4, H-5 and H-6 were ambiguous due to extensive overlap with the neighboring protons. Thus, the HSQC (Fig. 1(C-4)) and HMBC (Fig. 1(C-5)) were used to distinguish these ambiguously assigned protons. In addition, the ^{1}H chemical shifts in other four residues were also assigned by these spectra.

The ^{13}C NMR spectrum of SCPP11 was shown in Fig. 1(C-2). From spectrum, there were five signals in the anomeric region (δ 90–105 ppm), the signals were assigned to residues C (δ 91.88 ppm), D (δ 95.90 ppm), B (δ 98.90 ppm), A (δ 99.75 ppm) and E (δ 104.36 ppm) from the high field to the downfield, respectively, which were confirmed by cross-peaks in the ^{1}H–^{13}C HSQC spectrum. Based on the chemical shifts of protons, the carbon chemical shifts from C-1 to C-6 of residue A, B, C, D and E were identified from the HSQC spectrum and the results were summarized in Table 2. From the carbon chemical shifts, the downfield shifts of the C-1 (δ 99.75 ppm) and C-4 (δ 72.84 ppm) were confirmed that residue A was a 1,4-disubstituted α-D-Glc*p*. The downfield shift of C-1 with reference respect to standard value and no carbon signal was evident in the δ 76–82 indicating that residue B was substituted at C-1 (Ye et al., 2009). In addition, the downfield shifts of C-1, C-3, and C-6, C-1 and C-4, C-1 and C-6 carbon signals also indicated that residue C, D, E was α-1,4,6-D-Gal*p*, β-1,4-D-Gal*p* and β-1,6-D-Man*p*, respectively.

The HMBC spectrum was used to deduce the sequence of SCPP11 and confirm the assignments made from the HMQC. Residue A had inter-residue correlations from C-1 to H-6 and H-4 of residue C and H-4 of residue A indicated that residue A was linked at the 6-position and 4-position of residue C and 4-position A. Residue D had inter-residue correlations from C-1 to H-4 of residue A, indicating that residue D was linked at the 4-position of residue A. Similarly, residue E had inter-residue correlations C-1 to H-4 of residue D, revealing that residue E was linked at the 4-position of

Table 2
Chemical shift (δ) assignments of ^{1}H NMR and ^{13}C NMR spectra of SCPP11 on the basis of COSY, HSQC and HMBC.

Residues		The chemical shift of ^{1}H and ^{13}C (ppm)					
		1	2	3	4	5	6
(A)→1)-α-D-glc*p*-(4→	H	5.31	3.48	3.75	3.62	3.78	3.89
	C	99.75	71.29	72.68	72.84	71.47	60.73
(B) β-D-Glc*p*-(1→	H	4.87	3.49	3.74	3.57	3.78	3.75
	C	98.90	71.47	72.84	70.26	72.68	61.54
(C)→1)-α-D-Gal*p*-(4,6→	H	5.14	3.57	3.65	3.87	3.57	3.74
	C	91.88	72.84	72.21	76.69	73.63	71.17
(D)→1)-β-D-Gal*p*-(4→	H	4.51	3.57	3.68	4.03	3.68	3.74
	C	95.90	71.66	72.68	77.65	71.75	60.99
(E)→1)-β-D-Man*p*-(6→	H	4.53	3.58	3.74	4.05	3.63	3.74
	C	104.36	74.52	70.26	77.11	76.21	69.94

residue D. In addition, the residue C was linked at the 6-position of residue E.

Therefore, based on the chemical and spectroscopic findings, the predicted primary structure of the SCPP11 was established as shown in Fig. 1(D).

3.3. Molecular conformation

The HPSEC–MALL–RI system was used to determine the molecular conformation of SCPP11. The chromatogram based on the 90° light scattering and RI signals were shown in Fig. 2(A), it shown the two peaks are of similar sizes and shapes and almost completely overlaid, which suggests the interdetector delay procedure has been correctly determined when the system is properly aligned. The M_w, M_n and M_z of SCPP11 were 1.794×10^4, 1.162×10^4 and 1.489×10^4, respectively. Weight-average mean square radius (R_w), number-average mean square radius (R_n) and z-average mean square radius (R_z) were 11, 39 and 241 nm, respectively. The polydispersity index M_w/M_n was 1.543, which indicated that SCPP11 was a relatively homogeneous polysaccharide. The molecular conformation of the polymer molecules was also derived from the light scattering gradient based on the plot of $\langle r_g^2 \rangle_z^{1/2}$ as a function of M_w (Fig. 2(B)). Usually, the gradient values of 0.33, 0.50–0.60 and 1.0 reflect the polymer molecular shape as sphere, random coil and rigid rod, respectively (Huang, Huang, Li, & Zhang, 2009) (Tao, Zhang, & Zhang, 2009). The gradient value in Fig. 2(B) was 0.39, which indicated that a globular conformation with random coil structure.

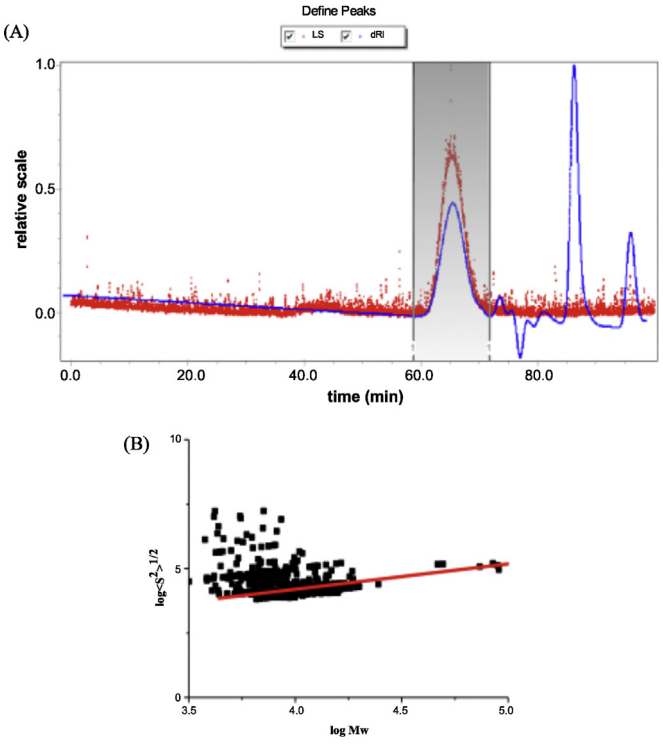

Fig. 2. (A) SEC and LLS chromatograms of SCPP11 in 0.1 mol/L NaCl at room temperature detected by laser light scattering photometry and differential refractometer. The detector 11 and AUX values are signals from the LLS at 90° and the refractive index detector. (B) The conformational plot (RMS radius versus molar mass) for the SCPP11 determined by the HPSEC-MALLS-RI system; the slope of the conformation plot is 0.39.

The conformation changes of SCPP11 induced by the temperature, pH value, ionic strength, Urea and Congo red could be detected by circular dichroism and the CD spectrums were summarized in Fig. 3. In Fig. 3(A), SCPP11 was influenced more, as was seen by comparing the signals at 25 °C with those at 60 and 100 °C. There was a peak maximum at 198 nm and minimum at about 196 nm and 202 nm, indicating the influence of ordered structures. At higher temperatures, at 100 °C, the maximum peak was displaced to 193 nm, and the minimum was displaced to 201 nm, indicating the chain extension and the remarkable transformation in conformation. In Fig. 3(B), compared with the SCPP11 in neutral solution, significant changes appeared in 190–220 nm of polysaccharides dissolved in acidic and alkaline solution, respectively. Positive Cotton effect appeared at 198 nm in acidic solution and negative cotton effect appeared at 194 nm and 217 nm in alkaline solution, indicating remarkable transformation in conformation. From Fig. 3(C), under the presence of Ca^{2+}, there were obvious positive cotton effect at 193 nm and 203 nm, showing the conformational change of SCPP11 and indicating that the complexes were formed between SCPP11 and Ca^{2+}. In Fig. 3(D), under Urea treatment, there are four obvious positive cottons at 193 nm, 203 nm, 210 nm and 216 nm, which indicated that the inter- and intramolecular hydrogen bonds of SCPP11 were destroyed by Urea. From Fig. 3(E), when treated with Congo red solution, the obvious positive cotton signals of SCPP11 were appeared at 193 nm, indicating the complexes were form between SCPP11 and Congo red and revealing the presence of ordered structures.

3.4. Molecular morphology

To provide direct evidence of the chain conformation of the SCPP11, AFM and TEM were used to observe their morphology. Fig. 4(A) showed the AFM image of the SCPP11 in pure water at room temperature and 100 °C, respectively. From Fig. 4(A-1), the individual agglomerated particles were dispersed in the dilute aqueous solution, which were in agreement with that determined by HPSEC–MALL–RI. The heights of the particle were in the range of 1–5 nm observed by AFM. The AFM image in Fig. 4(A-2) was the molecular morphology of SCPP11 through heating treatment at 100 °C. It shown the number of agglomerated

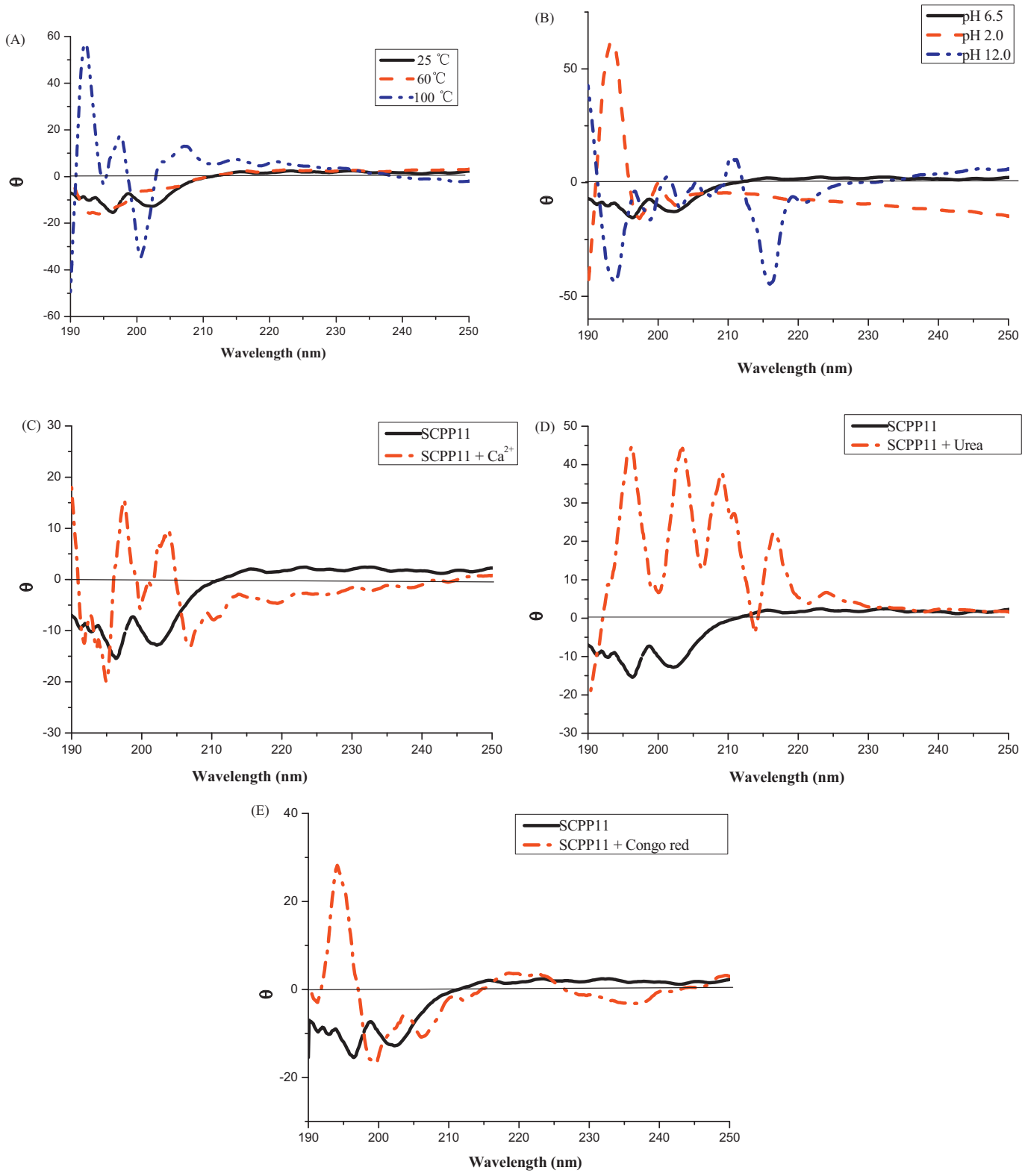

Fig. 3. The circular dichroism spectra of the SCPP11 at 1 mg/mL. The determination were recorded with a Jasco-810-150s instrument in the wavelength region from 190 to 250 nm. (A) Circular dichrosim spectra of the SCPP11 at different temperature (25, 60, 100 °C). (B) Circular dichrosim spectra of the SCPP11 at different pH values (pH: 2.0, 6.5, 12.0). (C) Circular dichrosim spectra comparison between SCPP11 and SCPP11 + Ca^{2+}. (D) Circular dichrosim spectra comparison between SCPP11 and SCPP11 + Urea. (E) Circular dichrosim spectra comparison between SCPP11 and SCPP11 + Congo red.

particles decreased dramatically and a large number of extended chains were distributed on the freshly cleaved mica. These chains height were observed in the range of 0.3–4 nm while the height of a single polysaccharide chain is generally 0.1–1 nm, which suggested molecular aggregation happened somehow during the drying process. Moreover, the changes of molecular morphology with different temperature treatment were coincided with the results of circular dichroism. Meanwhile, the agglomerated

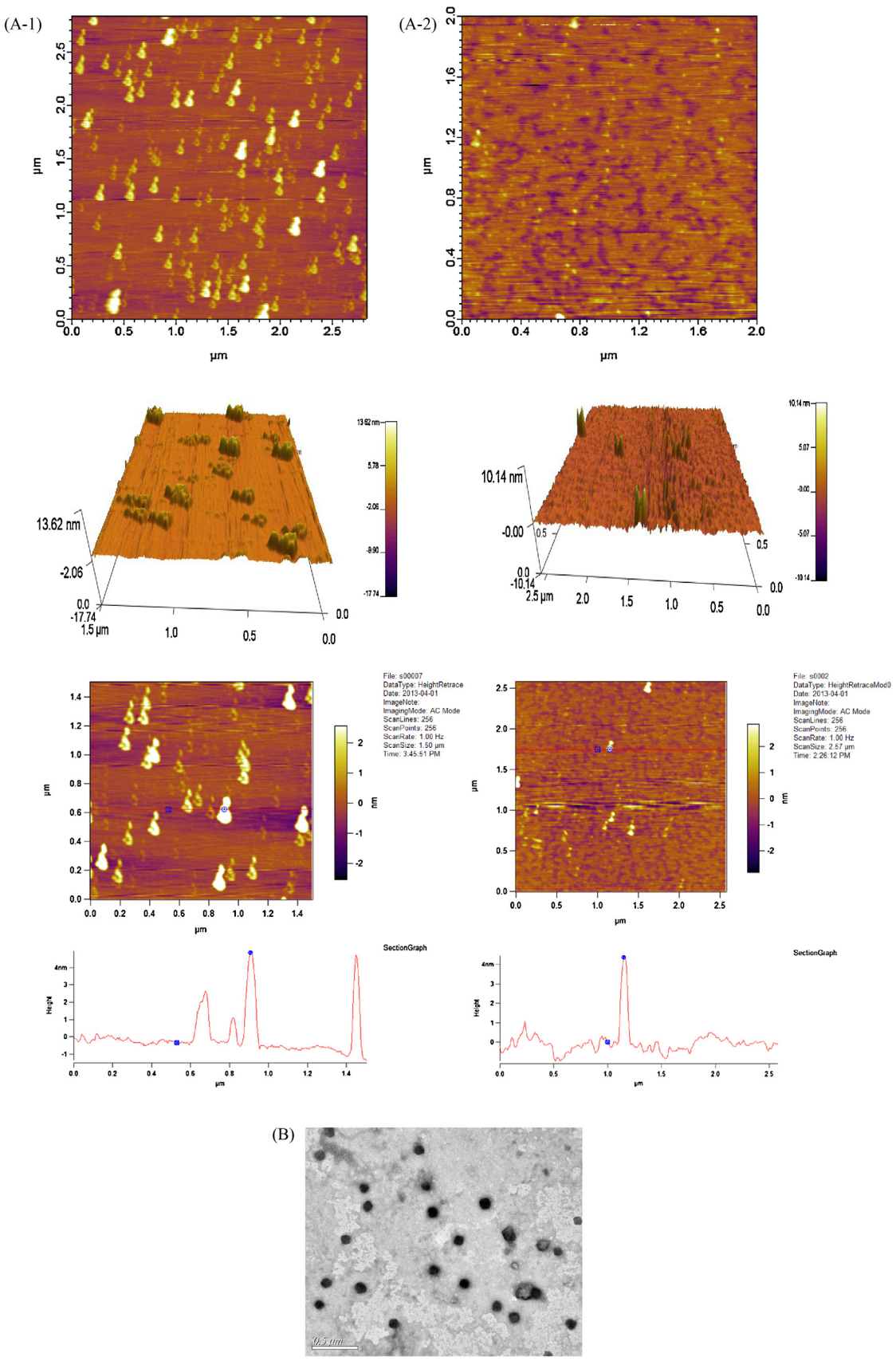

Fig. 4. (A) The AFM images of SCPP11 treated by different temperature (25 and 100 °C) were obtained with a MFP-3D atomic force microscope and collected by tapping mode. All measurement was performed in the air at ambient pressure and humidity. (B) TEM image of SCPP11 in distilled water was obtained by a high-resolution transmission electron microscope (JEM-2100, JEOL, Tokyo, Japan). The 0.2% phosphotungstic acid was used for staining.

conformation of SCPP11 indicated its branching structure and flexibility of chain.

TEM technology is widely used to observe and measure the morphology and dimension of particles including macromolecules (Tao & Xu, 2008). Fig. 4(B) shows the TEM images of SCPP11 in water. The agglomerated particles of SCPP11 exist in the dilute solution. The diameters of the particles by TEM were in the range of 100–200 nm.

3.5. Structure–activity correlation

Our previous study (Zao, Mao, Mao, et al., 2013) indicated that SCPP11 from *S. chinensis* (Turcz.) Baill exhibited non-cyctotoxic activity against HepG-2 tumor cells, but could significantly inhibit the growth of Heps tumor *in vivo* and could improve immune function in Heps-bearing mice. In the recent study, there are many polysaccharides with antitumor and immunomodulatory properties had been revealed, and these activities mainly depend on their structure including molecular weight, chemical composition, structure of the backbone, degree of branching, conformation and so on (Cui et al., 2007; Jin et al., 2003). Although it is difficult to clarify the structure–activity correlation of polysaccharide, some possible relationships could be deduced. It is noteworthy that polysaccharides with excellent antitumor and immunomodulatory activities are mostly heteropolysaccharides with low molecular (Gan, Ma, Jiang, Xu, & Zeng, 2011; Sun, Wang, & Zhou, 2012). In the present study, the SCPP11 possessed low molecular and three different monosaccharides, which might be regarded as two important factors related to the antitumor and immunomodulatory of SCPP11. Meanwhile, the study conducted by Yunmian He indicated that the branches in polysaccharide from *Arca subcrenata Lischke* were an extremely important factor for its immunololgical activity (He et al., 2007). It is interested that there are also branches in the main chain of SCPP11. In addition, the conformation of polysaccharides might be related to their antitumor and immunomodulatory properties. Polysaccharide from *Pleurotus tuber-regium* with sphere conformation showed potent in vitro antitumor activities (Tao et al., 2009). Phosphorylate (1-3)-β-D-gulcan from *Poria cocos* with more extended chain conformation were more beneficial to enhance its anti-tumor activity as a result of the increasing the chance of binding with receptors on the immune cells (Chen, Xu, Zhang, & Zeng, 2009). In the present study, SCPP11 have agglomerated conformation, branching structure, flexibility of chain and excellent antitumor and immunomodulatory activities. The results also indicated the recognition of biological systems for polysaccharides and the selection of bioactive polysaccharide.

4. Conclusions

On the basis of the previously results, the structure and conformation of SCPP11 were systematically elucidated for the first time. The repeating unit of SCPP11 was found to be a backbone composed of, 7.85% →1)-D-gal*p*-(4→linkages, 62.34% →1)-D-glu*p*-(4→linkages, 5.92% →1)-D-man*p*(6→linkages and 11.95% →1)-D-gal*p*-(4,6→linkages, and with a single branch at the C-4 position of gal according methylation analysis and NMR analysis. The conformation of SCPP11 was characterized as a globular conformation with seldom random coil of ordered structures in 0.1 M NaCl solution and evidences observed by AFM and TEM. The conformations of the SCPP11 were relative to their branched structures and flexibility of chain, and they might be the key factors for SCPP11 to exert excellent antitumor and immunomodulatory activities. The chemical structural modification and further structure–activity relationships would be investigated in the future.

Acknowledgments

This work was supported financially by Natural Science Fund of Jiangsu Province (BK2012702). We also appreciate Dr. Mohammed Takase and Dr. Samuel Jerry Cobbine for language polishing.

References

Carpita, N. C., & Shea, E. M. (1989). Linkage structure of carbohydrates by gas chromatography–mass spectrometry (GC–MS) of partially methylated alditol acetates. *Analysis of Carbohydrates by GLC and MS*, 157–216.

Chen, X., Xu, X., Zhang, L., & Zeng, F. (2009). Chain conformation and anti-tumor activities of phosphorylated (1 → 3)-β-D-glucan from *Poria cocos*. *Carbohydrate Polymers*, *78*(3), 581–587.

Chen, Y., Tang, J., Wang, X., Sun, F., & Liang, S. (2012). An immunostimulatory polysaccharide (SCP-IIa) from the fruit of *Schisandra chinensis* (Turcz.) Baill. *International Journal of Biological Macromolecules*, *50*(3), 844–848.

Cui, F. J., Tao, W. Y., Xu, Z. H., Guo, W. J., Xu, H. Y., Ao, Z. H., et al. (2007). Structural analysis of anti-tumor heteropolysaccharide GFPS1b from the cultured mycelia of *Grifola frondosa* GF9801. *Bioresource Technology*, *98*(2), 395–401.

Gan, D., Ma, L., Jiang, C., Xu, R., & Zeng, X. (2011). Production, preliminary characterization and antitumor activity in vitro of polysaccharides from the mycelium of *Pholiota dinghuensis* Bi. *Carbohydrate Polymers*, *84*(3), 997–1003.

Gao, X., Meng, X., Li, J., & Tong, H. (2009). Isolation, characterization and hypoglycemic activity of an acid polysaccharide isolated from *Schisandra chinensis* (Turcz.) Baill. *Letters in Organic Chemistry*, *6*(5), 428–433.

Han, X.-Q., Wu, X.-M., Chai, X.-Y., Chen, D., Dai, H., Dong, H.-L., et al. (2011). Isolation, characterization and immunological activity of a polysaccharide from the fruit bodies of an edible mushroom, *Sarcodon aspratus* (Berk.) S. Ito. *Food Research International*, *44*(1), 489–493.

He, Y., Liu, C., Chen, Y., Ji, A., Shen, Z., Xi, T., et al. (2007). Isolation and structural characterization of a novel polysaccharide prepared from *Arca subcrenata Lischke*. *Journal of Bioscience and Bioengineering*, *104*(2), 111–116.

Huang, Z., Huang, Y., Li, X., & Zhang, L. (2009). Molecular mass and chain conformations of *Rhizoma Panacis Japonici* polysaccharides. *Carbohydrate Polymers*, *78*(3), 596–601.

Jin, Y., Zhang, L., Zhang, M., Chen, L., Keung Cheung, P. C., Oi, V. E. C., et al. (2003). Antitumor activities of heteropolysaccharides of *Poria cocos* mycelia from different strains and culture media. *Carbohydrate Research*, *338*(14), 1517–1521.

Needs, P. W., & Selvendran, R. R. (1993). Avoiding oxidative degradation during sodium hydroxide/methyl iodide-mediated carbohydrate methylation in dimethyl sulfoxide. *Carbohydrate Research*, *245*(1), 1–10.

Pan, D., Wang, L., Chen, C., Teng, B., Wang, C., Xu, Z., et al. (2012). Structure characterization of a novel neutral polysaccharide isolated from *Ganoderma lucidum* fruiting bodies. *Food Chemistry*, *135*(3), 1097–1103.

Scoparo, C. T., de Souza, L. M., Rattmann, Y. D., Dartora, N., Paiva, S. M. M., Sassaki, G. L., et al. (2013). Polysaccharides from green and black teas and their protective effect against murine sepsis. *Food Research International*, *53*(2), 780–785.

Sheng, Y., Liu, Y., Huang, X., Yuan, G., & Guan, M. (2011). Purification, chemical characterization and in vitro antioxidant activities of alkali-extracted polysaccharide fractions isolated from the fruits of *Schisandra chinensis*. *Journal of Medicinal Plants Research*, *5*(24), 5881–5888.

Sun, L., Wang, L., & Zhou, Y. (2012). Immunomodulation and antitumor activities of different-molecular-weight polysaccharides from *Porphyridium cruentum*. *Carbohydrate Polymers*, *87*(2), 1206–1210.

Tao, Y., & Xu, W. (2008). Microwave-assisted solubilization and solution properties of hyperbranched polysaccharide. *Carbohydrate Research*, *343*(18), 3071–3078.

Tao, Y., Zhang, Y., & Zhang, L. (2009). Chemical modification and antitumor activities of two polysaccharide–protein complexes from *Pleurotus tuber-regium*. *International Journal of Biological Macromolecules*, *45*(2), 109–115.

Tong, H., Zhao, B., Du, F., Tian, D., Feng, K., & Sun, X. (2012). Isolation and physicochemical characterization of polysaccharide fractions isolated from *Schisandra chinensis*. *Chemistry of Natural Compounds*, *47*(6), 969–970.

Yang, L. Q., Zhao, T., Wei, H., Zhang, M., Zou, Y., Mao, G. H., et al. (2011). Carboxymethylation of polysaccharides from *Auricularia auricula* and their antioxidant activities *in vitro*. *International Journal of Biological Macromolecules*, *49*(5), 1124–1130.

Ye, L., Zhang, J., Yang, Y., Zhou, S., Liu, Y., Tang, Q., et al. (2009). Structural characterisation of a heteropolysaccharide by NMR spectra. *Food Chemistry*, *112*(4), 962–966.

Zhao, T., Mao, G., Mao, R., Zou, Y., Zheng, D., Feng, W., et al. (2013). Antitumor and immunomodulatory activity of a water-soluble low molecular weight polysaccharide from *Schisandra chinensis* (Turcz.) Baill. *Food and Chemical Toxicology*, *55*(0), 609–616.

Zhao, T., Mao, G. H., Zhang, M., Li, F., Zou, Y., Zhou, Y., et al. (2013). Anti-diabetic effects of polysaccharides from ethanol-insoluble residue of *Schisandra chinensis* (Turcz.) Baill on alloxan-induced diabetic mice. *Chemical Research in Chinese Universities*, *29*(1), 99–102.